

A comparison of analytic and numerical results for a two-dimensional control model in electromagnetic induction – I. *B*-polarization calculations

J. T. Weaver[★], B. V. Le Quang and G. Fischer
Observatoire Cantonal, CH-2000 Neuchâtel, Switzerland

Accepted 1985 January 15. Received 1985 January 15; in original form 1984 July 17

Summary. A conducting slab of finite thickness divided into three segments of different conductivities and overlying a perfect conductor is proposed as a suitable two-dimensional ‘control’ model for testing the accuracy of the various numerical modelling programs that are available for calculating the fields induced in the Earth by an external, time-varying magnetic source. An analytic solution is obtained for this control model for the case of the magnetic field everywhere parallel to the conductivity boundaries (*B*-polarization). Values of the field given by this solution for a particular set of model parameters are calculated at selected points on the surface and on a horizontal plane inside the conductor, and are tabulated to three figure accuracy for reference. They are used to check the accuracy of the results given by the finite difference program of Brewitt-Taylor & Weaver and the finite element program of Kisk & Silvester for the same model. Improved formulae for calculating the derived electric field components in *B*-polarization are first developed for incorporation in the finite difference program, and these give surface electric fields within 1 per cent of the analytic values, while all three field components inside the conductor are calculated to better than 96 per cent accuracy by the finite difference program. The results given by the finite element program are not quite so satisfactory. Errors somewhat greater than 10 per cent are present and although the program requires much less disk space it takes rather more CPU time to complete the calculations.

1 Introduction

There are many computer programs now available for calculating numerically the electromagnetic response of a 2-D model of the Earth to an external, time harmonic magnetic source which is usually considered to be locally uniform and horizontal. The various programs have been developed quite independently and have been based on several different

[★] On leave from the Department of Physics, University of Victoria, PO Box 1700, Victoria, BC V8W 2Y2, Canada.

methods – finite difference, finite element, integral equation and transmission line analogy, for example. An international project, designated COMMEMI, in which the numerical results given by these various programs applied to a number of standard models will be collected and compared, has recently been proposed and organized by Professor M. S. Zhdanov of Moscow.

It is desirable to include among these standard models at least one ‘control’ model which can also be solved analytically. After all, if the numerical results given by different computer programs differ from each other there is no knowing which (if any) of the programs is giving the correct solution and even if two programs do yield the same numerical solution this does not prove conclusively that it is, in fact, an accurate one. A modelling program should at least give results in good agreement with the analytic solution of a simple control model before it is applied to more complicated structures and subjected to a comparison with other programs.

Not a great deal of work has been done on developing such control models largely because of the paucity of analytic solutions presently available. To our knowledge the most detailed investigation of this type has been carried out by Klügel (1976). He compared the results given by a finite difference program (Losecke & Müller 1975) with the classical *B*-polarization solution of d’Erceville & Kunetz (1962) for the two-plate model – actually the thickness of the plates was taken to be several skin depths so that, in effect, the model investigated was the quarter-space shown in Fig. 1(a). He also compared the corresponding *E*-polarization calculations with what can be called a ‘quasi-analytic’ solution of the two-plate model obtained by a method of successive approximations first proposed by Weidelt (1966). Recently Doucet & Pham Van Ngoc (1984) have also used the quarter-space model to compare the surface values of apparent resistivity and phase for a *B*-polarization field as given by their own program, by another finite difference program and by the analytic solution of d’Erceville & Kunetz (1962). However, their investigation and conclusions were somewhat marred by the fact that they appeared to be unaware of algebraic errors in the finite difference program they were using in this comparison (Weaver 1985).

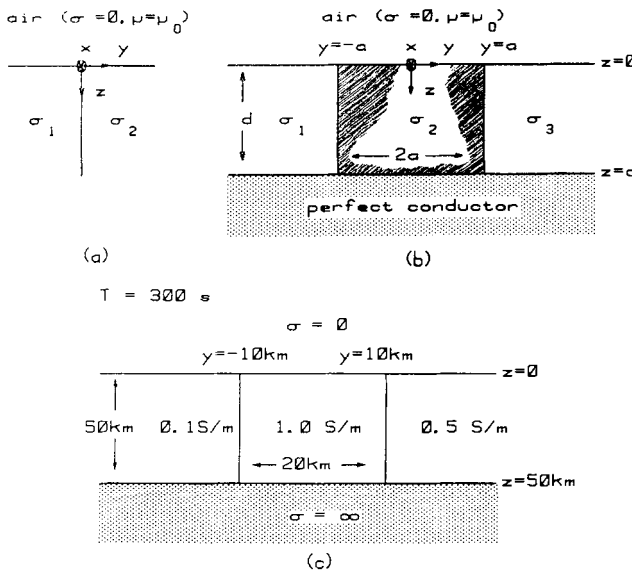


Figure 1. (a) The quarter-space model; (b) the control model proposed in this paper; (c) the particular reference model used in the comparison of analytic and numerical calculations.

In this paper we propose the use of a slightly more general control model in which the plate is divided into three, rather than two, different conductive segments overlying a perfect conductor. Such a model can be adapted to represent a variety of configurations which are useful for testing different computer programs, and we regard this greater flexibility as well worth the price of the increased complexity of the analytic solutions. The proposed model closely resembles the 'segmented overburden' model of Wait & Spies (1974) – also discussed by Wait (1982) – the only difference being that they took the basement to be a perfect insulator rather than a perfect conductor. Their method of solution is readily adapted to the proposed control model and the relevant analytic formulae are derived in Section 3 of this paper. Numerical values of the field components at selected points in a particular version of the control model have been generated by these formulae and are tabulated in Section 4 in the hope that they will provide a reference against which the B -polarization results of different computer programs may be checked.

We have begun this exercise here by comparing the tabulated values with the output given by (i) the finite difference program of Brewitt-Taylor & Weaver (1976) and (ii) the finite element program of Kisak & Silvester (1975) for the same control model. An improved method for calculating the derived fields in (i) has been incorporated in the program and is fully described in Section 5.

The derivation, by a method of successive approximations, of the quasi-analytic solution for the same model with an E -polarization field is a very much more involved exercise. Consequently we defer a comparison of the corresponding E -polarization calculations to a subsequent paper in which the development of the quasi-analytic solution will also be presented.

2 The control model

The model we have chosen is illustrated in Fig. 1(b). Referred to a rectangular coordinate system (x, y, z) it consists of a conducting plate of thickness d occupying the region $0 < z < d$ with an underlying perfect conductor at $z = d$. The plate is divided into three segments $y < -a$, $|y| < a$ and $y > a$ of conductivities σ_1 , σ_2 and σ_3 respectively. The half-space $z < 0$ is taken to be a perfect insulator and vacuum permeability μ_0 is assigned everywhere. The field vectors are assumed to be independent of the variable x and to have a time dependence $\exp(i\omega t)$ where ω is sufficiently small that displacement currents can be neglected. Then for the B -polarization field under consideration in this paper the spatial parts of the electric and magnetic fields may be written in the component form

$$\mathbf{E}(y, z) = (0, V, W), \quad \mathbf{B}(y, z) = (X, 0, 0).$$

In a medium of conductivity σ these components satisfy the Maxwell equations

$$\partial X / \partial z = \mu_0 \sigma V, \quad \partial X / \partial y = -\mu_0 \sigma W, \quad i\omega X = \partial V / \partial z - \partial W / \partial y, \quad (1)$$

from which it can be deduced that for constant σ

$$\partial^2 X / \partial y^2 + \partial^2 X / \partial z^2 = i\alpha^2 X \quad (2)$$

where $\alpha^2 = \omega\mu_0\sigma$. A subscript j ($j = 1, 2, 3$) on the field components and the parameters α and σ will be used to denote their different values in the three different segments.

The control model described above offers the following advantages:

(i) It includes such well-known models as the dyke ($\sigma_1 = \sigma_3$), the vertical fault ($\sigma_2 = \sigma_3$), and the quarter-space ($\sigma_2 = \sigma_3, d \rightarrow \infty$) as special cases.

(ii) the effect of both high and low conductivity contrasts can be examined in the same model choosing (say) $\sigma_2/\sigma_1 > 10$, $1 < \sigma_2/\sigma_3 < 5$.

(iii) Programs which can only deal with 'anomalous' regions of finite horizontal extent embedded in a 'normal' 1-D structure can also be tested by putting $\sigma_1 = \sigma_3$ in the control model.

(iv) With $\sigma_1 < \sigma_2 < \sigma_3$ (or $\sigma_1 > \sigma_2 > \sigma_3$) and $2a$ chosen small so that it equals the node separation in a numerical grid, the control model can be used to check the accuracy of the numerical solution for a model in which the conductivity changes gradually from one value (σ_1) to the next (σ_3) over a transition zone comprising three successive cells – normally only simple conductivity contrasts can be considered.

(v) The perfect conductor at finite depth d provides a clean cut-off to the numerical model and permits the use of a reasonably small grid (with consequent savings in CPU time) when testing programs against the control model.

3 The analytic solution

The method of solution is so similar to that of Wait & Spies (1974), which was itself a straightforward extension of the solutions of d'Erceville & Kunetz (1962) and Rankin (1962), that it will be only outlined here. We note first that equations (1) give the familiar result $X = B_0$ (a constant) in the non-conducting region $z < 0$. Thus X_j ($j = 1, 2, 3$), must satisfy (2) (with $\alpha = \alpha_j$) in the j th segment subject to the boundary conditions:

- (i) $X_j = B_0$ on $z = 0$;
- (ii) $\partial X_j / \partial z = 0$ on $z = d$;
- (iii) $X_1 = X_2$ and $\sigma_2 \partial X_1 / \partial y = \sigma_1 \partial X_2 / \partial y$ on $y = -a$;
- (iv) $X_2 = X_3$ and $\sigma_3 \partial X_2 / \partial y = \sigma_2 \partial X_3 / \partial y$ on $y = +a$.

These follow directly from the continuity of the tangential electric and magnetic fields at a boundary and the vanishing of the tangential electric field at the surface of a perfect conductor.

Now the general solution of (2) in the j th segment can clearly be written in the form

$$X_j = B_0 \frac{\cosh [(d - z) \alpha_j \sqrt{i}]}{\cosh (d \alpha_j \sqrt{i})} + f_j(y, z), \quad (3)$$

where the particular integral represented by the first term is a 1-D solution of (2) that already satisfies boundary conditions (i) and (ii). Thus f_j is a solution of (2) which can be found by separation of the variables and which satisfies $f_j = 0$ on $z = 0$ and $\partial f_j / \partial z = 0$ on $z = d$. The z -dependent part of f_j can therefore be expressed as a Fourier sine series in z , and the full solution takes the form

$$f_1(y, z) = \sum_{m=0}^{\infty} P_m \exp(y \gamma_m^{(1)}) \sin(k_m z) \quad (4)$$

$$f_2(y, z) = \sum_{m=0}^{\infty} [Q_m \exp(y \gamma_m^{(2)}) + R_m \exp(-y \gamma_m^{(2)})] \sin(k_m z) \quad (5)$$

$$f_3(y, z) = \sum_{m=0}^{\infty} S_m \exp(-y \gamma_m^{(3)}) \sin(k_m z) \quad (6)$$

where P_m, Q_m, R_m and S_m are coefficients to be determined and

$$k_m = (2m + 1) \pi / 2d, \quad \gamma_m^{(j)} = \sqrt{k_m^2 + i\alpha_j^2}. \tag{7}$$

The key to applying the remaining boundary conditions (iii) and (iv) at $y = \pm a$ rests with the possibility of finding the Fourier series expansion

$$\frac{\cosh [(d - z) \alpha_j \sqrt{i}]}{\cosh (d \alpha_j \sqrt{i})} - \frac{\cosh [(d - z) \alpha_2 \sqrt{i}]}{\cosh (d \alpha_2 \sqrt{i})} = \sum_{m=0}^{\infty} K_m^{(j)} \sin (k_m z) \tag{8}$$

for $j = 1, 3$. The standard integration formula for calculating Fourier coefficients gives

$$K_m^{(j)} = \frac{2ik_m (\alpha_2^2 - \alpha_j^2)}{d (\gamma_m^{(2)} \gamma_m^{(j)})^2}. \tag{9}$$

Thus when the boundary conditions (iii) and (iv) are applied to the solutions (3), and the substitutions (4), (5), (6) and (7) are made, four equations are found which specify that four different Fourier sine series are identically vanishing. Equating the coefficients in these series to zero we obtain four equations which can be solved for the four unknowns P_m, Q_m, R_m and S_m . These are then substituted back into (4), (5) and (6) and after some algebraic rearrangement the solution (3) can be put into the form

$$\frac{X_j}{B_0} = \frac{\cosh [(d - z) \alpha_j \sqrt{i}]}{\cosh (d \alpha_j \sqrt{i})} + \sum_{m=0}^{\infty} F_m^{(j)}(y) \sin (k_m z) \tag{10}$$

where

$$F_m^{(1)}(y) = \beta_m^{(1)} A_m^{(1)} \exp [(a + y) \gamma_m^{(1)}] \tag{11}$$

$$F_m^{(2)}(y) = (A_m^{(1)} - C_m^{(1)}) \exp [(a + y) \gamma_m^{(2)}] + (A_m^{(3)} - C_m^{(3)}) \exp [(a - y) \gamma_m^{(2)}] \tag{12}$$

$$F_m^{(3)}(y) = \beta_m^{(3)} A_m^{(3)} \exp [(a - y) \gamma_m^{(3)}]. \tag{13}$$

Here we have defined for $j = 1, 3$

$$A_m^{(j)} = \frac{2 \exp (-2a \gamma_m^{(2)})}{D_m} \{ \bar{K}_m^{(j)} - K_m^{(j)} [\cosh (2a \gamma_m^{(2)}) + \bar{\beta}_m^{(j)} \sinh (2a \gamma_m^{(2)})] \}, \tag{14}$$

$$C_m^{(j)} = [(1 - \beta_m^{(j)}) \bar{K}_m^{(j)} \exp (-2a \gamma_m^{(2)}) - (1 + \bar{\beta}_m^{(j)}) K_m^{(j)}] / D_m, \tag{15}$$

where

$$\beta_m^{(j)} = \frac{\gamma_m^{(2)} / \sigma_2}{\gamma_m^{(j)} / \sigma_j}, \quad \bar{\beta}_m^{(j)} = \frac{\beta_m^{(1)} \beta_m^{(3)}}{\beta_m^{(j)}}, \quad \bar{K}_m^{(j)} = \frac{K_m^{(1)} K_m^{(3)}}{K_m^{(j)}}, \tag{16}$$

and

$$D_m = (1 + \beta_m^{(1)})(1 + \beta_m^{(3)}) - (1 - \beta_m^{(1)})(1 - \beta_m^{(3)}) \exp (-4a \gamma_m^{(2)}). \tag{17}$$

The electric field components are obtained from (10) by differentiation according to the Maxwell equations (1). Thus we have

$$\frac{V_j}{B_0} = -\frac{\omega}{\alpha_j} \left[\frac{\sqrt{i} \sinh [(d - z) \alpha_j \sqrt{i}]}{\cosh (d \alpha_j \sqrt{i})} - \frac{1}{\alpha_j} \sum_{m=0}^{\infty} k_m F_m^{(j)}(y) \cos (k_m z) \right], \tag{18}$$

$$\frac{W_j}{B_0} = -\frac{\omega}{\alpha_2^2} \sum_{m=0}^{\infty} \gamma_m^{(2)} G_m^{(j)}(y) \sin (k_m z), \tag{19}$$

where

$$G_m^{(1)}(y) = A_m^{(1)} \exp [(a + y) \gamma_m^{(1)}], \quad G_m^{(3)}(y) = -A_m^{(3)} \exp [(a - y) \gamma_m^{(3)}],$$

$$G_m^{(2)}(y) = (A_m^{(1)} - C_m^{(1)}) \exp [(a + y) \gamma_m^{(2)}] - (A_m^{(3)} - C_m^{(3)}) \exp [(a - y) \gamma_m^{(2)}].$$

4 A particular reference model

The solutions (10), (18) and (19) have been programmed for numerical calculation and we present here the field values obtained at selected points for the particular model shown in Fig. 1(c) in the hope that these will serve as at least an initial standard against which the results given by various computer programs can be compared. As shown in the figure the parameters used in this calculation were $T \equiv 2\pi/\omega = 300$ s, $a = 10$ km, $d = 50$ km, $\sigma_1 = 0.1 S m^{-1}$, $\sigma_2 = 1.0 S m^{-1}$ and $\sigma_3 = 0.5 S m^{-1}$. Note that the skin depths in the three regions from left to right are respectively 27.6, 8.7 and 12.3 km. This makes the width of the central segment just over two skin depths while the thickness of the left segment is just under two skin depths.

Since the magnetic field is constant and the vertical electric field is vanishing along the

Table 1. Values of the field components calculated from the analytic solution for selected points on the surface $z = 0$ and the interior plane $z = 15$ km of the reference model shown in Fig. 1(c). The values of V/B_0 and W/B_0 are given in units of $V m^{-1} T^{-1}$.

	y (km)	X/B_0		V/B_0		W/B_0	
		Re	Im	Re	Im	Re	Im
$z = 0$ km							
	-52	1	0	-308	-292	0	0
	-25	1	0	-322	-287	0	0
	-15	1	0	-348	-303	0	0
	-10-	1	0	-379	-366	0	0
	-10+	1	0	-37.9	-36.6	0	0
	- 7	1	0	-59.4	-85.1	0	0
	0	1	0	-83.4	-99.1	0	0
	7	1	0	-82.1	-92.8	0	0
	10-	1	0	-74.6	-75.3	0	0
	10+	1	0	-149	-151	0	0
	15	1	0	-138	-130	0	0
	30	1	0	-129	-128	0	0
	50	1	0	-129	-129	0	0
$z = 15$ km							
	-52	.461	-.311	-247	-66.6	.363	-2.88
	-25	.443	-.298	-250	-56.8	15.8	-2.66
	-15	.412	-.300	-253	-44.9	37.0	7.69
	-10-	.383	-.307	-252	-30.5	55.2	17.7
	-10+	.383	-.307	-25.2	-3.05	55.2	17.7
	- 7	.205	-.341	-23.2	6.30	39.2	2.06
	0	8.50×10^{-4}	-.302	-19.6	16.0	9.81	-6.46
	7	-3.82×10^{-3}	-.263	-20.0	16.7	-7.54	-2.21
	10-	3.64×10^{-2}	-.257	-21.8	14.6	-13.8	-1.54
	10+	3.64×10^{-2}	-.257	-43.7	29.1	-13.8	-1.54
	15	7.07×10^{-2}	-.256	-46.5	25.6	-8.32	.847
	30	.104	-.271	-48.5	22.9	-.746	1.34
	50	.104	-.279	-48.9	22.6	.152	9.02×10^{-2}

surface $z = 0$ we have computed the values of all the field components at points along the surface $z = 15$ km inside the conductor as well as values of the horizontal electric field along the surface $z = 0$. Table 1 gives the field for various values of y on the two surfaces. Although the series were summed until adding an extra term gave a relative change of less than 10^{-6} per cent, the values in Table 1 are given to three significant figures only since this is the best that can be reasonably expected from the results obtained by the numerical methods discussed in Section 6.

5 Improved derivative formulae for finite difference calculations

In Section 6 we shall compare the analytic solution of the reference model just discussed with the corresponding results given by the finite difference program of Brewitt-Taylor & Weaver (1976). In their original program the derived field components were calculated by central differences at the centre of the cells in the numerical mesh rather than at the nodes themselves. This certainly preserved the accuracy of the calculations but was an undesirable feature of the program since different components of the same electromagnetic field were then computed at separate points. For example it would clearly be inconvenient to make the sort of comparison envisaged in this paper if the values of the electric field were not obtained at the same points as those of the magnetic field.

One way round this difficulty, of course, is simply to obtain the nodal values of the derived field by three-point interpolation, but problems with this procedure arise at conductivity boundaries where the normal electric field is discontinuous. Instead we have developed a method for computing the electric field components at the nodes themselves using nothing more than the same central difference approximations that were required in the derivation of the B -polarization finite difference equations for the magnetic field. The method is briefly outlined in this section and the final formulae are stated in a form that is easily coded for inclusion in a computer program.

We remind the reader that Brewitt-Taylor & Weaver (1976) showed that in a 1-D model the central difference formula for the magnetic field at a node between two layers of different resistivities was the same whether the node was assumed to be on a sharp boundary between the two layers or in a transition zone in which the resistivity varied from one value to the other in such a way that the resistivity at the node itself was a weighted average of the values in the two layers. The latter interpretation is particularly useful for the extension to higher dimensions because it is obvious how to make the appropriate generalization of the weighted average resistivity at the nodes of a 2- or 3-D grid. We stress, however, that the dual interpretation remains valid. Thus in a 2-D model where the resistivity varies in both the y - and z -directions, it matters not whether we regard a grid point $y = y_m, z = z_n$ as lying (i) on a sharp boundary $y = y_m$ with the resistivity varying across a transition zone in the z -direction, or (ii) on a sharp boundary $z = z_n$ with variable resistivity in the y -direction, or (iii) in a 2-D transition zone with the appropriately weighted average resistivity assigned to the node. The same finite difference equation for the magnetic field X is obtained in each case. For reasons discussed at length by Brewitt-Taylor & Weaver (1976) it is not possible to regard both $y = y_m$ and $z = z_n$ as sharp boundaries simultaneously.

Retaining the notation of Brewitt-Taylor & Weaver (1976), we define $\rho = 1/\alpha^2$, which is proportional to the resistivity, and note that if the conductivity in Maxwell's equations (1) is a function of position rather than a constant, then instead of (2) we have

$$\frac{\partial^2 X}{\partial y^2} + \frac{\partial^2 X}{\partial z^2} + \frac{1}{\rho} \frac{\partial \rho}{\partial y} \frac{\partial X}{\partial y} + \frac{1}{\rho} \frac{\partial \rho}{\partial z} \frac{\partial X}{\partial z} = -X. \quad (20)$$

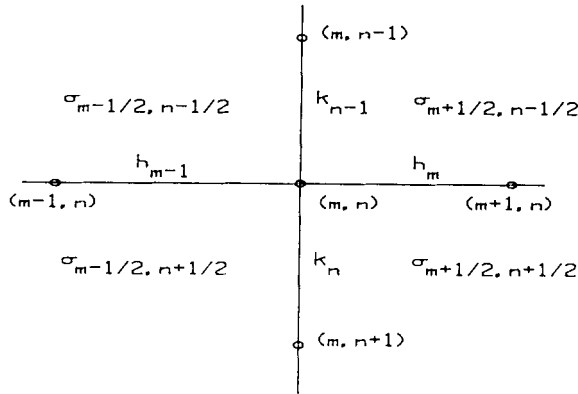


Figure 2. The general node (m, n) in the numerical grid for finite difference calculations.

The node at the point (y_m, z_m) is labelled (m, n) , the distances to neighbouring nodes to the left, right, top and bottom of (m, n) are denoted by h_{m-1} , h_m , k_{n-1} and k_n respectively, and the conductivities in the four adjacent cells are $\sigma_{m\pm 1/2, n\pm 1/2}$ as shown in Fig. 2. The corresponding parameters ρ are labelled likewise. The weighted average values of ρ at the points $(y_m, z_n - k_{n-1}/2)$, $(y_m, z_n + k_n/2)$, $(y_m - h_{m-1}/2, z_n)$ and $(y_m + h_m/2, z_n)$ are written as $\rho_{m, n-1/2}$, $\rho_{m, n+1/2}$, $\rho_{m-1/2, n}$ and $\rho_{m+1/2, n}$ respectively, where

$$\rho_{m, n\pm 1/2} = \frac{h_{m-1}\rho_{m-1/2, n\pm 1/2} + h_m\rho_{m+1/2, n\pm 1/2}}{h_m + h_{m-1}} \quad (21)$$

$$\rho_{m\pm 1/2, n} = \frac{k_{n-1}\rho_{m\pm 1/2, n-1/2} + k_n\rho_{m\pm 1/2, n+1/2}}{k_n + k_{n-1}} \quad (22)$$

and the value at the node (m, n) itself is taken to be

$$\rho_{m, n} = \frac{k_n\rho_{m, n+1/2} + k_{n-1}\rho_{m, n-1/2}}{k_n + k_{n-1}}. \quad (23)$$

The required finite difference expressions for the electric field components are obtained by expanding X in a Taylor series (up to and including second-order terms) horizontally and vertically about the node (m, n) . For an expansion parallel to the y -axis the plane $y = y_m$ is treated as a sharp boundary (interpretation (i) above) across which the normal electric field V is discontinuous whenever $\rho_{m-1/2, n} \neq \rho_{m+1/2, n}$. The two one-sided values of this field are denoted by $V_{m-, n}$ and $V_{m+, n}$ respectively; the other field component $W_{m, n}$ is, of course, uniquely defined on $y = y_m$ because it is tangential to the boundary. It is the normal component of the current density $\mathbf{j} = \mathbf{E}/\omega\mu_0\rho$ which is continuous across $y = y_m$, and the uniquely defined value of $(j_y)_{m, n}$ on $y = y_m$ is related to the two values of the discontinuous electric field by the equations

$$V_{m-, n}/\rho_{m-1/2, n} = V_{m+, n}/\rho_{m+1/2, n} = \omega\mu_0(j_y)_{m, n}. \quad (24)$$

On the other hand we have $(j_z)_{m-, n} \neq (j_z)_{m+, n}$ in general because the continuity of W

requires that

$$\rho_{m-1/2, n}(j_z)_{m-, n} = \rho_{m+1/2, n}(j_z)_{m+, n} = \rho_{m, n}(j_z)_{m, n} \text{ (say)}. \quad (25)$$

The last term in (25) serves as a suitable definition of $(j_z)_{m, n}$ when we switch to interpretation (ii) in which $z = z_n$ is the sharp boundary and the resistivity varies smoothly in the y -direction across a transition zone about $y = y_m$. In this case, corresponding to (24) and (25), W and j_y are discontinuous across $z = z_n$ in such a way that

$$W_{m, n-}/\rho_{m, n-1/2} = W_{m, n+}/\rho_{m, n+1/2} = \omega\mu_0(j_z)_{m, n} \quad (26)$$

and

$$\rho_{m, n-1/2}(j_y)_{m, n} = \rho_{m, n+1/2}(j_y)_{m, n} = \rho_{m, n}(j_y)_{m, n} \text{ (say)}. \quad (27)$$

Thus the pair of equations (24), (25) are used with interpretation (i), and the pair (26), (27) with interpretation (ii), while the definitions of $(j_y)_{m, n}$ and $(j_z)_{m, n}$ in (27) and (25) provide the connection between the two interpretations.

Taylor expansions of X to the left and right of (m, n) with its (discontinuous) first derivative in y related to j_z through the second of Maxwell's equations (1) and equation (26), and its second derivative in y eliminated with the aid of (20) in which $\partial\rho/\partial y = 0$ (since $y = y_m$ is being regarded as a sharp boundary separating two regions whose resistivities are locally independent of y) yield two equations each containing a term involving $(\partial^2 X/\partial z^2)_{m, n}$. When this term is eliminated we obtain a single equation which, after considerable algebraic simplification, gives the result

$$(j_z)_{m, n} = \frac{\rho_{m+1/2, n}\rho_{m-1/2, n}L_{m, n}}{\mu_0(h_m + h_{m-1})\rho_{m, n}^2} \quad (28)$$

where

$$\begin{aligned} L_{m, n} = & \frac{h_m}{h_{m-1}} X_{m-1, n} - \frac{h_{m-1}}{h_m} X_{m+1, n} - M_{m, n} \left(\frac{k_n}{k_{n-1}} X_{m, n-1} - \frac{k_{n-1}}{k_n} X_{m, n+1} \right) \\ & + \left[\frac{h_{m-1}}{h_m} - \frac{h_m}{h_{m-1}} + M_{m, n} \left(\frac{k_n}{k_{n-1}} - \frac{k_{n-1}}{k_n} \right) \right. \\ & \left. + \frac{ih_m h_{m-1}}{2} \left(\frac{1}{\rho_{m, n-1/2}} - \frac{1}{\rho_{m, n+1/2}} \right) \right] X_{m, n} \end{aligned} \quad (29)$$

and

$$\begin{aligned} M_{m, n} = & \frac{h_m h_{m-1}}{(k_n + k_{n-1})^2} \left[\frac{\rho_{m-1/2, n+1/2} - \rho_{m-1/2, n-1/2}}{\rho_{m-1/2, n}} \right. \\ & \left. - \frac{\rho_{m+1/2, n+1/2} - \rho_{m+1/2, n-1/2}}{\rho_{m+1/2, n}} \right]. \end{aligned} \quad (30)$$

Similarly, expansions of X up and down from the node (m, n) lead to the result

$$(j_y)_{m, n} = \frac{\rho_{m, n+1/2}\rho_{m, n-1/2}N_{m, n}}{\mu_0(k_n + k_{n-1})\rho_{m, n}^2} \quad (31)$$

with

$$\begin{aligned}
 N_{m,n} = & \frac{k_{n-1}}{k_n} X_{m,n+1} - \frac{k_n}{k_{n-1}} X_{m,n-1} - O_{m,n} \left(\frac{h_{m-1}}{h_m} X_{m+1,n} - \frac{h_m}{h_{m-1}} X_{m-1,n} \right) \\
 & + \left[\frac{k_n}{k_{n-1}} - \frac{k_{n-1}}{k_n} + O_{m,n} \left(\frac{h_{m-1}}{h_m} - \frac{h_m}{h_{m-1}} \right) + \frac{ik_n k_{n-1}}{2} \right. \\
 & \left. \times \left(\frac{1}{\rho_{m,n-1/2}} - \frac{1}{\rho_{m,n+1/2}} \right) \right] X_{m,n}, \quad (32)
 \end{aligned}$$

$$O_{m,n} = \frac{k_n k_{n-1}}{(h_m + h_{m-1})^2} \left[\frac{\rho_{m+1/2,n-1/2} - \rho_{m-1/2,n-1/2}}{\rho_{m,n-1/2}} - \frac{\rho_{m+1/2,n+1/2} - \rho_{m-1/2,n+1/2}}{\rho_{m,n+1/2}} \right]. \quad (33)$$

Formulae (28) and (31) are used in conjunction with (24) and (26) to compute the components of the electric field at each interior node (m, n) . If $\rho_{m-1/2,n} = \rho_{m+1/2,n}$ the two one-sided values of V become identical, i.e. $V_{m-,n} = V_{m+,n} = V_{m,n}$, and likewise if $\rho_{m,n-1/2} = \rho_{m,n+1/2}$ it follows from (26) that $W_{m,n-} = W_{m,n+} = W_{m,n}$.

The nodes on the surfaces $z = 0$ require special consideration because for B -polarization modelling they are at the top of the numerical grid and only downwards Taylor expansion is possible. On the surface itself we know from boundary condition (i) in Section 3 that $X_{m,1} = B_0$, a constant, for all values of m . Thus the downwards expansion of the field together with substitution from the first Maxwell equation (1) and the differential equation (20) gives

$$X_{m,2} = \left(1 + \frac{ik_1^2}{2\rho_{m,3/2}} \right) B_0 + \mu_0 k_1 (j_y)_{m,1} \quad (34)$$

all other terms, which involve y -derivatives of the field, having vanished because X is constant along the surface. It follows from (24) that

$$\frac{V_{m-,1}}{\rho_{m-1/2,3/2}} = \frac{V_{m+,1}}{\rho_{m+1/2,3/2}} = \frac{\omega}{k_1} (X_{m,2} - B_0) - \frac{i\omega k_1 B_0}{2\rho_{m,3/2}}. \quad (35)$$

This agrees with the special formula derived by Brewitt-Taylor & Weaver (1976) except that they took the weighted average value

$$V_{m,1} = \frac{h_{m-1} V_{m-,1} + h_m V_{m+,1}}{h_m + h_{m-1}}$$

for the electric field at $(m, 1)$.

Formula (26) for the vertical electric field is, of course, replaced by $W_{m,1} = 0$ at the surface, a result which follows at once from the second of Maxwell's equations (1) and the constancy of X on $z = 0$.

6 Numerical calculations

The particular reference model described in Section 4 has been used to test two numerical modelling programs. Field values have been calculated at the same selected points shown in Table 1 using (i) the finite difference program of Brewitt-Taylor & Weaver (1976) modified to include the improved derivative formulae developed in the preceding section, and (ii) the

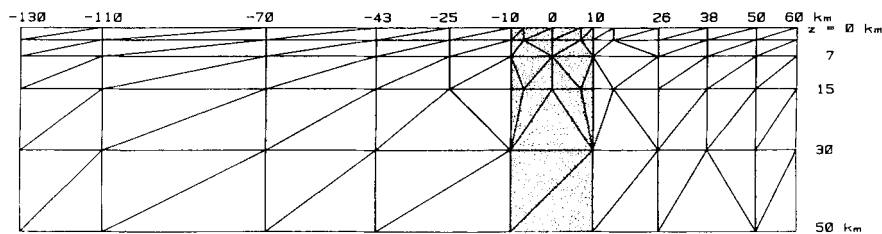


Figure 3. Triangulation of the region $z > 0$ for finite element calculations.

finite element program of Kisak & Silvester (1975) which is obtainable from the CPC Program Library at Queen's University in Belfast.

For the finite difference calculations a 35×16 numerical grid was used with nodes at $y = -130, -110, -90, -80, -70, -61, -52, -43, -34, -25, -19, -15, -12, -10, -8.5, -7, -5, -2.5, 0, 2.5, 5, 7, 8.5, 10, 12, 15, 18, 22, 26, 30, 34, 38, 43, 50, 60$ km, and $z = 0, 1.5, 3, 5, 7.5, 10, 12.5, 15, 17.5, 20, 24, 28, 32, 40, 45, 50$ km. The triangulation of the region $z > 0$ for the application of the finite element program is shown in Fig. 3. Two nodes were taken along the sides and one in the centre of each triangle in addition to those

Table 2. As in Table 1 except that the field components are calculated by the finite difference program of Brewitt-Taylor & Weaver (1976).

z (km)	y (km)	X/B_0		V/B_0		W/B_0	
		Re	Im	Re	Im	Re	Im
z = 0 km	-52	1	0	-307	-291	0	0
	-25	1	0	-320	-287	0	0
	-15	1	0	-346	-302	0	0
	-10-	1	0	-376	-362	0	0
	-10+	1	0	-37.6	-36.2	0	0
	-7	1	0	-58.9	-86.6	0	0
	0	1	0	-82.8	-100	0	0
	7	1	0	-81.5	-94.1	0	0
	10-	1	0	-74.0	-75.3	0	0
	10+	1	0	-148	-151	0	0
	15	1	0	-137	-131	0	0
	30	1	0	-129	-129	0	0
	50	1	0	-128	-130	0	0
z = 15 km	-52	0.462	-0.308	-247	-65.6	0.514	-2.74
	-25	0.444	-0.296	-250	-56.3	16.4	-1.88
	-15	0.413	-0.298	-253	-45.0	37.3	8.38
	-10-	0.384	-0.306	-252	-31.0	55.3	18.3
	-10+	0.384	-0.306	-25.2	-3.10	55.3	18.3
	-7	0.206	-0.340	-23.4	6.12	39.3	2.62
	0	2.46×10^{-3}	-0.300	-19.9	15.6	10.1	-6.24
	7	-2.73×10^{-3}	-0.262	-20.3	16.2	-7.37	-2.26
	10-	3.68×10^{-2}	-0.255	-22.1	14.2	-13.6	-1.63
	10+	3.68×10^{-2}	-0.255	-44.2	28.3	-13.6	-1.63
	15	7.06×10^{-2}	-0.255	-46.9	24.9	-8.27	0.745
	30	0.103	-0.270	-48.9	22.3	-0.798	1.31
	50	0.104	-0.277	-49.3	22.0	9.20×10^{-2}	0.239

at the vertices, making a total of 580 points at which the field was calculated. The CPU time required for these calculations on a VAX-780 computer was 50 s with the finite difference program and 90 s with the finite element program.

The values obtained by these two methods are tabulated in Tables 2 and 3 respectively in the same format as the analytic solutions given in Table 1. For a visual comparison of the results, the variations of the real and imaginary parts of V/B_0 across the surface $z = 0$, as given by the three different methods of calculation, are depicted in Fig. 4. The similarity between the finite difference curves and those based on the analytic solution is quite remarkable; in fact a comparison of the numerical values for $z = 0$ in Tables 1 and 2 indicates that the errors in the finite difference results are extremely small – maximum 1.5 per cent and generally under 1 per cent relative to typical electric field values in the region (i.e. the field at the left edge of the model for $y < -10$ km, at the right edge for $y > 10$ km, and the

Table 3. As in Table 1 except that the field components are calculated by the finite element program of Kisak & Silvester (1975). Where two values of the electric field on $z = 0$ are given, the point is at a common vertex of two of the triangular elements shown in Fig. 3, and the two values are derivatives associated with the two triangles. The values of the electric field components on the interior plane $z = 15$ km are not given by the finite element program.

$z = 0$ km	y (km)	X/B_0		V/B_0		W/B_0	
		Re	Im	Re	Im	Re	Im
	-52	1	0	-271	-280	0	0
	-25	1	0	-289	-278	0	0
	-15	1	0	-318	-300	0	0
	-10-	1	0	-344	-325	0	0
	-10+	1	0	-34.9	-35.4	0	0
	- 7	1	0	-57.7 -57.4	-87.0 -85.3	0	0
	0	1	0	-82.7 -83.0	-97.9 -99.9	0	0
	7	1	0	-82.3	-94.0 -93.2	0	0
	10-	1	0	-74.8	-78.9	0	0
	10+	1	0	-150	-151	0	0
	15	1	0	-138	-130	0	0
	30	1	0	-130	-128	0	0
	50	1	0	-129	-129	0	0
$z = 15$ km							
	-52	0.530	-0.281				
	-25	0.504	-0.277				
	-15	0.468	-0.284				
	-10-	0.437	-0.295				
	-10+	0.437	-0.295				
	- 7	0.246	-0.346				
	0	1.30×10^{-2}	-0.317				
	7	-4.22×10^{-3}	-0.271				
	10-	3.36×10^{-2}	-0.261				
	10+	3.36×10^{-2}	-0.261				
	15	6.71×10^{-2}	-0.259				
	30	0.102	-0.270				
	50	0.103	-0.278				

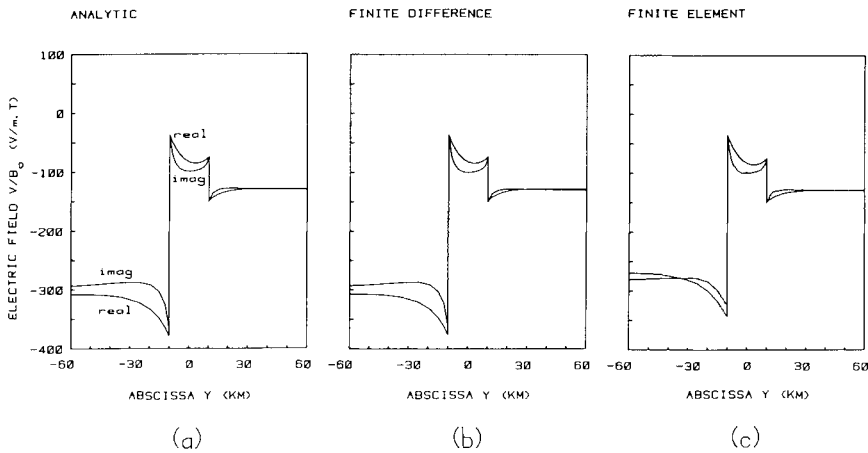


Figure 4. Comparison of the variations of the real and imaginary parts of the horizontal electric field V across the surface $z = 0$ of the model shown in Fig. 1(c), as given by (a) the analytic solution (b) the finite difference program of Brewitt-Taylor & Weaver (1976), and (c) the finite element program of Kisak & Silvester (1975).

field at $y = 0$ for $|y| < 10$ km). The finite element calculations are not quite so satisfactory. The field values for $y > -10$ km are in reasonably good agreement with the analytic solution but larger discrepancies occur over the plate of smallest conductivity in the region $y < -10$ km. The less smooth variation of the field depicted in Fig. 4(c) is a result of the finite element program giving two values for the derived field at those nodes which are at a common vertex of two triangles – one value for each triangle. In regions of uniform conductivity these two values should be the same but this did not always turn out to be the case in these particular model calculations. The different values obtained at some of the selected points are given in Table 3, where it will also be seen that errors somewhat greater than 10 per cent are present in the finite element calculations.

Only the calculated values of the derived field V can be compared on the surface $z = 0$. In order to test the accuracy of the magnetic field X , which is of course the component actually calculated by the finite difference and finite element programs, it is necessary to go to the interior of the conductor. In Fig. 5 the variations of all three components along the interior plane $z = 15$ km are depicted. Only the finite difference results for the electric field components are plotted alongside the analytic solutions because it is not possible, without modifying the program, to obtain the derived fields inside the conductor with the finite element program supplied by Kisak & Silvester (1975). The agreement between the two sets of curves is again visually quite striking; the behaviour of the fields as given by the analytic solutions plotted on the left is faithfully reproduced in every detail by the finite difference calculations. Reference to the numerical values given at the selected points in Tables 1 and 2 confirm that the errors in the magnetic field are less than 1 per cent (relative to B_0), and that the errors in the electric field components relative to typical values in the region are always less than 4 per cent and generally much less. Once again the finite element calculations (in this case for the magnetic field) are not so accurate with errors around 10 per cent occurring in the left segment.

We conclude that the finite difference program of Brewitt-Taylor & Weaver (1976), together with the improved derivative formulae developed in this paper, gives excellent results when applied to our control model and can therefore be used with some confidence

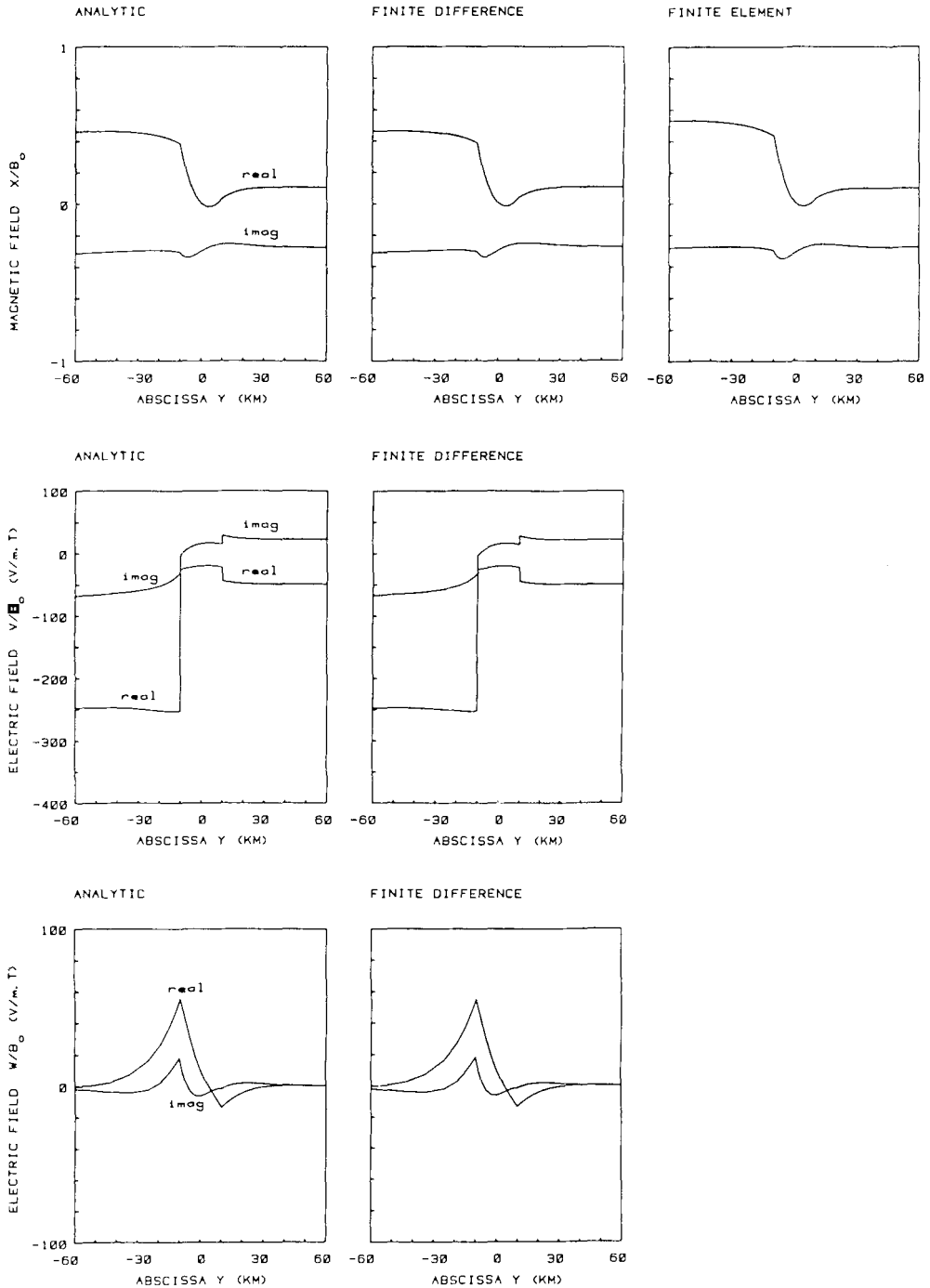


Figure 5. Comparison of the variations of the real and imaginary parts of the horizontal magnetic (X), horizontal electric (V) and vertical electric (W) fields along the plane $z = 15$ km inside the conducting slab shown in Fig. 1(c). The curves on the left were obtained from the analytic solution and those in the centre from the finite difference program of Brewitt-Taylor & Weaver (1976). Only the variation of X is given by the finite element program of Kisak & Silvester (1975) and is shown on the right.

in the numerical modelling of B -polarization induction problems. The finite element program of Kisak & Silvester (1975) is also acceptable but is less accurate, requires more CPU time (although less disk space), and is actually less convenient to use because the task of designing the numerical model is more time-consuming than for finite difference calculations. The real advantage of the finite element method lies in its ability to handle sloping conductivity boundaries, but such complications have not been considered in this paper.

More serious discrepancies between the two programs arise when they are applied to E -polarization models. A full discussion of these problems will be deferred to a subsequent paper in which the quasi-analytic E -polarization solution of the control model will also be developed.

Acknowledgments

The finite difference program used in this investigation was a new FORTRAN version of the original program (which had been partially written in IBM assembler language) developed under the supervision of Mr Jon DeLaurier at the Pacific Geoscience Centre, Victoria, BC. The assistance of Mr Adrian Dolling of the University of Victoria in further modifying the program to bring it into FORTRAN 77 form for implementation on the VAX computer and to include the new derivative formulae described in this paper is also acknowledged. This work was undertaken while one of us (JTW) was a visitor at the Observatoire Cantonal de Neuchâtel on leave from the University of Victoria. He wishes to thank the Swiss National Science Foundation and the Canton of Neuchâtel for the financial support which made this visit possible, and Dr Gaston Fischer, Associate Director of the Observatoire, and his colleagues for their hospitality during his stay. This research is supported by grants from the Swiss National Science Foundation, the Geophysical Commission of the Academy of Natural Sciences (Switzerland), and the Natural Sciences and Engineering Research Council of Canada.

References

- Brewitt-Taylor, C. R. & Weaver, J. T., 1976. On the finite difference solution of two-dimensional induction problems, *Geophys. J. R. astr. Soc.*, **47**, 375–396.
- Doucet, D. & Pham Van Ngoc, 1984. Généralisation et optimisation de la méthode des différences finies pour la modélisation en magnétotellurique (MT), *Geophys. Prospect.*, **32**, 292–316.
- d'Erceville, I. & Kunetz, G., 1962. Some observations regarding naturally occurring electromagnetic fields in applied geophysics, *Geophysics*, **27**, 651–665.
- Kisak, E. & Silvester, P., 1975. A finite element program package for magnetotelluric modelling, *Comput. Phys. Commun.*, **10**, 421–433.
- Klügel, M., 1976. Berechnung der elektromagnetischen Induktion in zwei Halbplatten zur Anwendung in der Magnetotellurik und erdmagnetischen Tiefensondierung, *Diplomarbeit*, Braunschweig, Techn. Univ., Inst. Geophys. Meteorol.
- Losecke, W. & Müller, W., 1975. Two-dimensional magnetotelluric model calculations for overhanging, high resistivity structures, *J. Geophys.*, **41**, 311–319.
- Rankin, D., 1962. The magneto-telluric effect on a dike, *Geophysics*, **27**, 666–676.
- Wait, J. R., 1982. *Geo-electromagnetism*, pp. 197–201, Academic Press, New York.
- Wait, J. R. & Spies, K. P., 1974. Magneto-telluric fields for a segmented overburden, *J. Geomagn. Geoelect.*, **26**, 449–458.
- Weaver, J. T., 1985. Comment on 'Généralisation et optimisation de la méthode des différences finies pour la modélisation en magnétotellurique (MT)' by D. Doucet and Pham Van Ngoc, *Geophys. Prospect.*, **33**, 303–307.
- Weidelt, P., 1966. Modellrechnungen zur Deutung der norddeutschen Leitfähigkeitsanomalie als oberflächennahe Leitfähigkeitsänderung, *Diplomarbeit*, University of Göttingen.